Supporting information

Thermocline depth and euphotic zone thickness regulate the abundance of diazotrophic cyanobacteria in Lake Tanganyika

Benedikt Ehrenfels[1,2], Maciej Bartosiewicz[3], Athanasio S. Mbonde[4], Kathrin B.L. Baumann[1,2], Christian Dinkel[1], Julian Junker[5,6], Tumaini Kamulali[4], Ismael A. Kimirei[4,7], Daniel Odermatt[1], Francesco Pomati[8], Emmanuel A. Sweke[4,9], Bernhard Wehrli[1,2]

[1]Eawag, Swiss Federal Institute of Aquatic Science and Technology, Department Surface Waters – Research and Management, Kastanienbaum, Switzerland
[2]ETH Zurich, Institute of Biogeochemistry and Pollutant Dynamics, Zurich, Switzerland
[3]University of Basel, Department of Environmental Sciences, Basel, Switzerland
[4]TAFIRI, Tanzania Fisheries Research Institute, Kigoma, Tanzania
[5]Eawag, Swiss Federal Institute of Aquatic Science and Technology, Department Fish Ecology and Evolution, Kastanienbaum, Switzerland
[6]University of Bern, Institute of Ecology & Evolution, Bern, Switzerland
[7]TAFIRI, Tanzania Fisheries Research Institute, Kigoma, Tanzania
[8]Eawag, Swiss Federal Institute of Aquatic Science and Technology, Department Aquatic Ecology, Dübendorf, Switzerland
[9]DSFA, Deep Sea Fishing Authority, Zanzibar, Tanzania

Correspondence to: Benedikt Ehrenfels (benedikt.ehrenfels@eawag.ch)

Contents

1 Sampling

1.1 Station information

Table S1: Station dates and coordinates of the two expeditions at the end of the dry season (Septemper/October 2017) and the end of the rainy season (April/May 2018).

	date	station	latitude [° N]	longitude [° E]
Sep/Oct 2017	28.09.2017	1	-4.50	29.47
	29.09.2017	2	-5.00	29.50
	30.09.2017	2	-5.00	29.50
	01.10.2017	3	-5.5	29.65
	02.10.2017	4	-6	29.6
	03.10.2017	5	-6.5	29.82
	04.10.2017	6	-6.92	30.22
	05.10.2017	7	-7.48	30.45
	06.10.2017	7	-7.48	30.45
	07.10.2017	8	-8	30.72
	08.10.2017	9	-8.52	31
Apr/May 2018	27.04.2018	1	-4.50	29.47
	28.04.2018	2	-5.00	29.50
	29.04.2018	2	-5.00	29.50
	30.04.2018	3	-5.5	29.65
	01.05.2018	4	-6	29.6
	02.05.2018	5	-6.5	29.82
	03.05.2018	6	-6.92	30.22
	04.05.2018	7	-7.48	30.45
	05.05.2018	7	-7.48	30.45
	06.05.2018	8	-8	30.72
	07.05.2018	9	-8.52	31

1.2 Phytoplankton community analyses

Table S2: List of taxa identified by microscopic phytoplankton community analyses.

Chlorophytes	Dinophytes	Euglenophytes	Diatoms	Cyanobacteria
Botrococcus braunii	*Glenodinium sp*	*Trachelomonas sp*	*Amphora sp*	*Dolichospermum flos-aquae*
Dictyosphaeria simplex	*Peridium sp*	*Trachelomonas volvocina*	*Aulacoseira sp*	*Dolichospermum spiroides*
Dictyosphaerium pulchellum			*Cyclotella sp*	*Dolichospermum sp*
Dictyosphaerium sp			*Cymbella sp*	*Anabaenopsis tanganyikae*
Gloeocystis sp			*Epithemia argus*	*Chroococcus dispersus*
Gloeocystis gigas			*Fragilaria sp*	*Chroococcus sp*
Oocystis lacustris			*Navicula sp*	*Microcystis flos-aquae*
Oocystis solitaria			*Nitzschia acicularis*	*Microcystis sp*
Oocystis sp			*Nitzschia asterionoides*	
Rhaphidinium sp			*Nitzschia sp*	
Scenedesmus sp			*Rhopalodia sp*	
Sphinctosiphon polymorphus			*Stephanodiscus sp*	
Spirogyra sp			*Surirella sp*	
Staurastrum sp			*Synedra sp*	

2 Additional information on the thermal structure of the water column

With the data at hand, we cannot identify the processes responsible for the formation of a deep, secondary thermocline in Sep/Oct (Table S3 & Fig. S1), but splitting of the thermocline may have resulted from surface and subsurface water currents flowing in opposite directions during this time of the year (Verburg et al., 2011). The surface thermocline in Apr/May might be 'seasonal' thermocline (Hecky et al., 1996) or biologically induced (see section 5).

Table S3: Depth and strength, measured as buoyancy frequency (N^2), of the thermocline and euphotic depth (z_{eu}) during the end of the dry season (September/October 2017) and the end of rainy season (April/May 2018). At some stations, secondary thermoclines had formed. The primary thermoclines separated nitrate-depleted surface water masses from underlying nitrate-rich waters as used in Fig. 1 & 3. The temperature profile of station 9 exhibited no thermocline.

		secondary surface thermocline		primary thermocline		secondary deep thermocline		
	station	depth [m]	N^2 [s^{-2}]	depth [m]	N^2 [s^{-2}]	depth [m]	N^2 [s^{-2}]	z_{eu} [m]
Sep/Oct 2017	1			34	2.13E-04	55	2.14E-04	
	2			38.5	2.31E-04	64	2.40E-04	
	3			36.5	1.66E-04	54.5	1.91E-04	
	4			50	1.78E-04	82.5	1.17E-04	
	5			43	1.96E-04	86	2.40E-04	
	6			53.5	2.68E-04	100	1.50E-04	
	7			38	1.89E-04	82.5	1.82E-04	
	8			17.5	1.81E-04			
	9			12*	1.50E-04*			
Apr/May 2018	1			44.5	2.41E-04	62.5	2.02E-04	54.8
	2			63.5	2.50E-04			46.8
	3	27.5	2.47E-04	58.5	4.20E-04			40.8
	4	30	1.11E-04	63.0	2.54E-04			51.8
	5			55.5	5.03E-04			46.8
	6			48.5	3.38E-04			46.8
	7			55.5	2.83E-04			51.3
	8			34.0	3.82E-04			51.3
	9			23.0	3.80E-04			35.8

* for station 9 (Sep/Oct), we indicated the depth and value of the N^2 maximum, even though there was no clear thermocline. These values were used for the quantitative analyses depicted in Fig. 4 & S3.

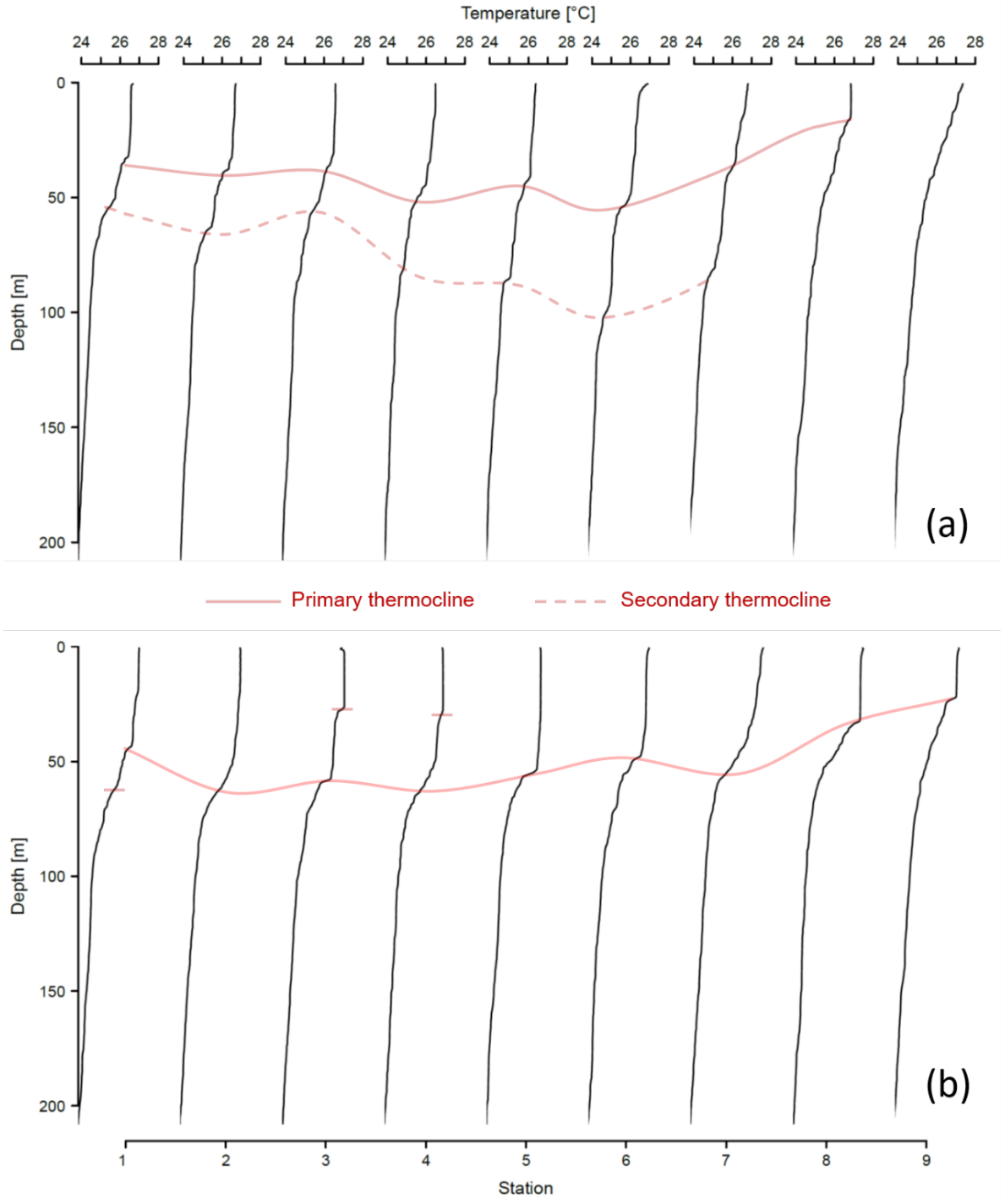

Figure S2: Temperature profiles of all 9 sampling stations during September/October 2017 **(a)** and April/May 2018 **(b)** including the approximate depths of the primary and secondary thermocline. The temperature profiles pertaining to April/May 2018 are also presented by C. Callbeck, B. Ehrenfels, K.B.L. Baumann, B. Wehrli, and C.J. Schubert (manuscript in review at *Nat. Comms.*).

3 Nitrogen deficit

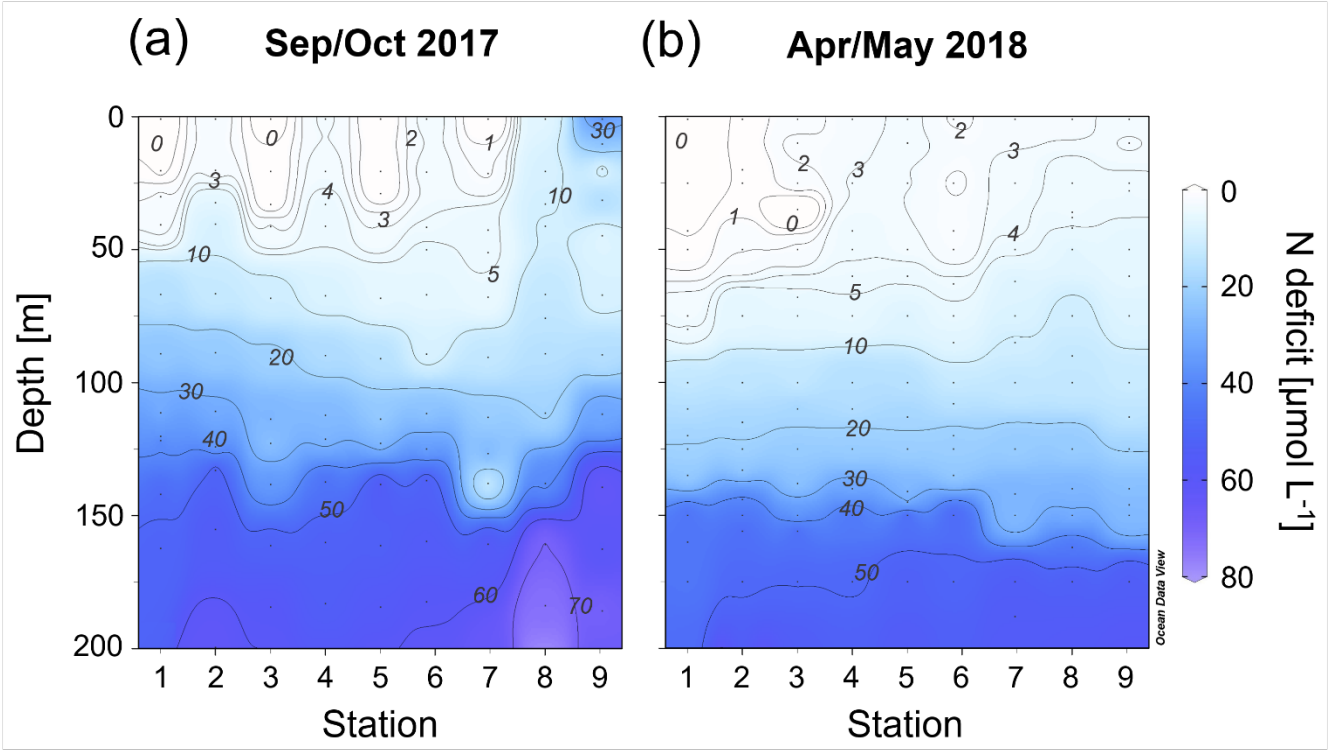

Figure S2: Contour plot showing the distribution of the nitrogen (N) deficit in Lake Tanganyika in a North-South transect (whereby station 1 is the northernmost and station 9 the southernmost station) during **(a)** the end of the dry season (September/October 2017) and **(b)** the end of the more stratified rainy season (April/May 2018). Dots indicate samples.

4 Depth-integrated pigment concentrations

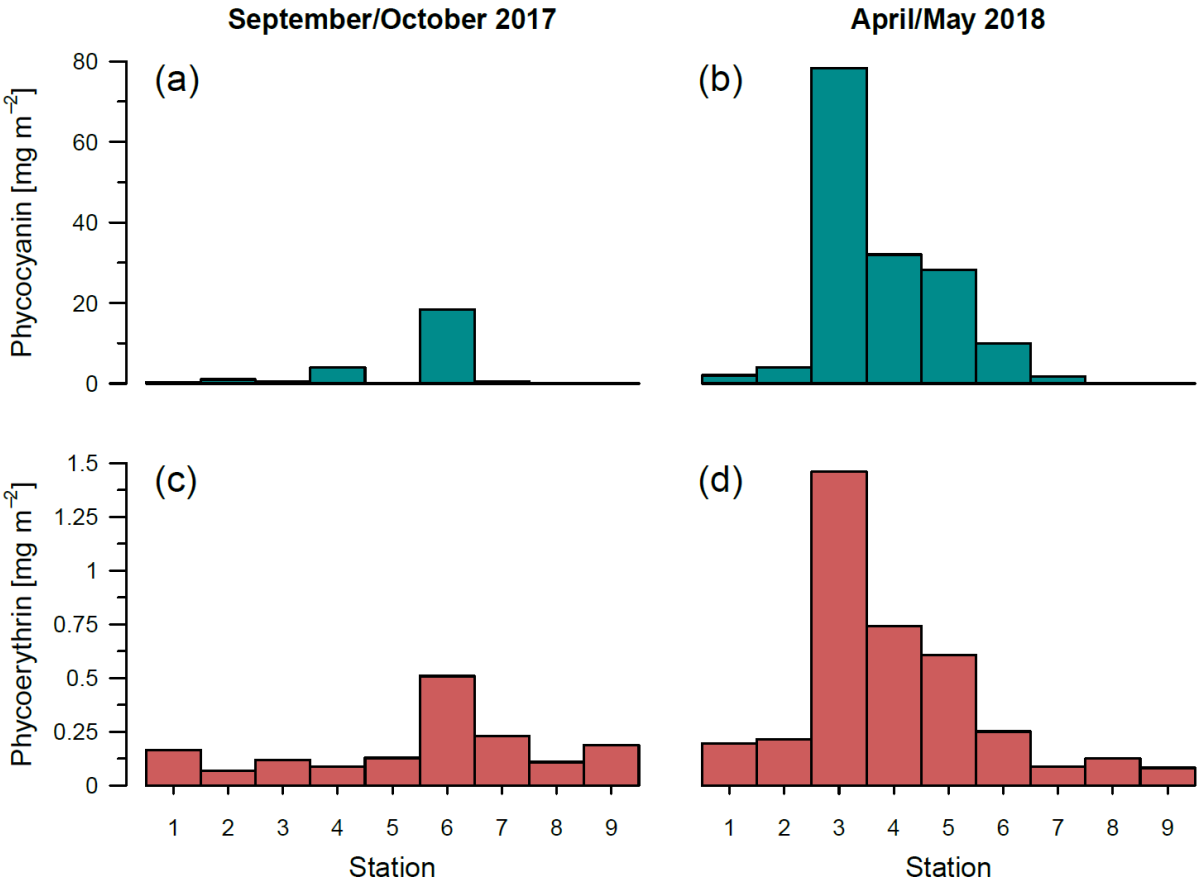

Figure S3: Depth integrated concentrations of the cyanobacterial pigments phycocyanin **(a,b)** and phycoerythrin **(c,d)** for the end of the dry season (September/October 2017) and the end of the rainy season (April/May 2018). We calculated the integrals from the water surface to 125 m depth, to include only photosynthetically active organisms from the oxygenated epi- and metalimnion.

5 River influence and surface thermocline

The presence of high NO_3^- concentrations during sampling at station 3 (one observation at 35 m) may have coincided with the presence of the Malagarasi river inflow. However, our biogeochemical profiles do not support this possibility as neither pH nor conductivity or dissolved organic carbon values (Fig. S4) in this water mass are indicative of the riverine inputs (Athuman and Nkotagu, 2013). We also expect that under severe N depletion in the upper water column any inflowing NO_3^- is consumed rapidly after entering surface waters.

Instead, we interpret this NO_3^- accumulation as regenerated DIN originating from the surface diazotroph-diatom-chlorophyte community. The high surface cell densities might have created a surface mixed layer that is marked by a near-surface thermocline just above the local NO_3^- peak at stations 3 and 4. The strengthening of thermal stratification by the enhanced light absorption of high cell densities is a well-known phenomenon (Edwards et al., 2004; Zhai et al., 2011). This "thermal shielding" (Bartosiewicz et al., 2019) in combination with bioconvetion (Nguyen-Quang and Guichard, 2010) of buoyant cyanobacteria may have created the surface mixed layer with constantly high temperatures of ~27 °C in contrast to the steady temperature gradients at the surrounding sites (Fig. S5), and might be responsible for the relatively shallow euphotic depth (40.8 m).

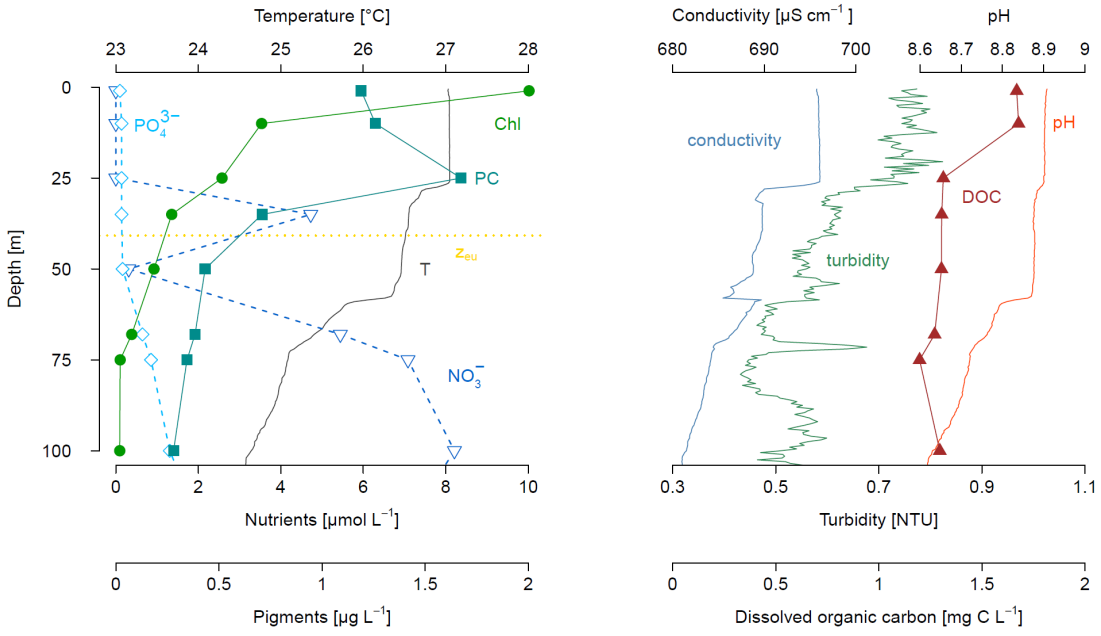

Figure S4: Vertical profiles of physical, biogeochemical and biological data from station 3 at the end of the rainy season (April/May 2018). The left panel shows temperature (T) and euphotic depth (z_{eu}) as well as the nitrate (NO_3^-), phosphate (PO_4^{3-}), chlorophyll (Chl), and phycocyanin (PC) concentrations, whereas the right panel exhibits conductivity, pH, turbidity and the dissolved organic carbon (DOC) concentrations.

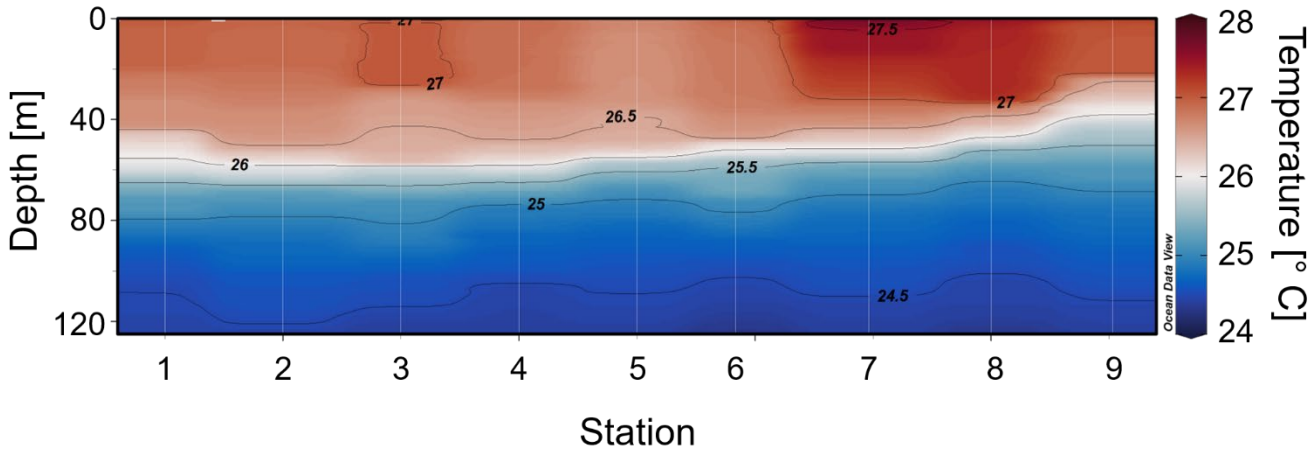

Figure S5: Contour plot of the temperature profiles in a North-South transect at the end of the rainy season (April/May 2018). White lines mark CTD profiles.

References

Athuman, C. B. and Nkotagu, H. H.: A Limnological Survey of Malagarasi River in Western Tanzania, Rwanda J., 1(1), 74–89, 2013.

Bartosiewicz, M., Przytulska, A., Deshpande, B. N., Antoniades, D., Cortes, A., MacIntyre, S., Lehmann, M. F. and Laurion, I.: Effects of climate change and episodic heat events on cyanobacteria in a eutrophic polymictic lake, Sci. Total Environ., 693(July), 133414, doi:10.1016/j.scitotenv.2019.07.220, 2019.

Edwards, A. M., Wright, D. G. and Platt, T.: Biological heating effect of a band of phytoplankton, J. Mar. Syst., 49(1–4), 89–103, doi:10.1016/j.jmarsys.2003.05.011, 2004.

Hecky, R. E., Bootsma, H. A., Mugidde, R. M. and Bugenyi, F. W. B.: Phosphorous Pumps, Nitrogen Sinks, and Silcon drains Plumbing Nutrients in the African Great Lakes, in The limnology, climatology and paleoclimatology of the East African lakes, pp. 205–233, Gordon and Breach Publishers, Amsterdam, Amsterdam., 1996.

Nguyen-Quang, T. and Guichard, F.: The role of bioconvection in plankton population with thermal stratification, Int. J. Bifurc. Chaos, 20(6), 1761–1778, doi:10.1142/S0218127410026812, 2010.

Verburg, P., Antenucci, J. P. and Hecky, R. E.: Differential cooling drives large-scale convective circulation in Lake Tanganyika, Limnol. Oceanogr., 56(3), 910–926, doi:10.4319/lo.2011.56.3.0910, 2011.

Zhai, L., Tang, C., Platt, T. and Sathyendranath, S.: Ocean response to attenuation of visible light by phytoplankton in the Gulf of St. Lawrence, J. Mar. Syst., 88(2), 285–297, doi:10.1016/j.jmarsys.2011.05.005, 2011.